

This PDF file is subject to the following conditions and restrictions:

Copyright © 2005, The Geological Society of America, Inc. (GSA). All rights reserved. Copyright not claimed on content prepared wholly by U.S. government employees within scope of their employment. Individual scientists are hereby granted permission, without fees or further requests to GSA, to use a single figure, a single table, and/or a brief paragraph of text in other subsequent works and to make unlimited copies for noncommercial use in classrooms to further education and science. For any other use, contact Copyright Permissions, GSA, P.O. Box 9140, Boulder, CO 80301-9140, USA, fax 303-357-1073, editing@geosociety.org. GSA provides this and other forums for the presentation of diverse opinions and positions by scientists worldwide, regardless of their race, citizenship, gender, religion, or political viewpoint. Opinions presented in this publication do not reflect official positions of the Society.

Chicxulub impact ejecta deposits in southern Quintana Roo, México, and central Belize

Kevin O. Pope*

Geo Eco Arc Research, 16305 St. Mary's Church Road, Aquasco, Maryland 20608, USA

Adriana C. Ocampo*

Jet Propulsion Laboratory, California Institute of Technology, 4800 Oak Grove Drive, Pasadena, California 91109, USA

Alfred G. Fischer

Department of Earth Sciences, University of Southern California, University Park, Los Angeles, California 90089, USA

Francisco J. Vega

Instituto de Geología, Universidad Nacional Autónoma de México, Ciudad Universitaria, México D.F. 04510, México

Doreen E. Ames

Geological Survey of Canada, Natural Resources Canada, 601 Booth Street, Ottawa, Ontario K1A 0E8, Canada

David T. King Jr.

Department of Geology, Auburn University, Auburn, Alabama 36849, USA

Bruce W. Fouke

Richard J. Wachtman

Department of Geology, University of Illinois at Urbana-Champaign, Urbana, Illinois 61801, USA

Gunther Kletetschka

Department of Physics, Catholic University of America, Washington D.C., USA; Institute of Geology, Academy of Sciences, Prague, Czech Republic, and NASA Goddard Space Flight Center, Greenbelt, Maryland 20771, USA

ABSTRACT

Discoveries of Chicxulub impact ejecta of the Albion Formation in road cuts and quarries in southern Quintana Roo, México and Belize, broaden our understanding of ejecta depositional processes in large impacts. There are numerous new exposures of ejecta near the Río Hondo in Quintana Roo México, located at distances of 330–350 km from the center of the Chicxulub crater. A single ejecta exposure was discovered near Armenia in central Belize, 470 km from Chicxulub. The Albion Formation is composed of two lithostratigraphic units: the spheroid bed and diamictite bed, originally identified at Albion Island, Belize. The new spheroid bed exposures range from

*E-mail, Pope: kpope@starband.net. *Note:* Pope and Ocampo contributed jointly to this paper.

Pope, K.O., Ocampo, A.C., Fischer, A.G., Vega, F.J., Ames, D.E., King, D.T., Jr., Fouke, B.W., Wachtman, R.J., and Kletetschka, G., 2005, Chicxulub impact ejecta deposits in southern Quintana Roo, México, and central Belize, in Kenkmann, T., Hörz, F., and Deutsch, A., eds., Large meteorite impacts III: Geological Society of America Special Paper 384, p. 171–190. For permission to copy, contact editing@geosociety.org. © 2005 Geological Society of America.

2 to 5 m thick and are composed of altered glass fragments, accretionary lapilli, and pebble-sized carbonate clasts in a fine-grained calcite matrix. The base of the spheroid bed is exposed at Ramonal South in México and at Albion Island and Armenia in Belize, and at all three locations, the spheroid bed was deposited on a weathered karst land surface that had emerged in the Late Cretaceous. The new diamictite bed exposures are composed of altered glass fragments and carbonate clasts up to 9.0×3.2 m in size. In all but one of the new exposures, the diamictite bed extends to the surface with observed thicknesses up to 8 m. At Agua Dulce in México, the weathered top of the diamictite bed is overlain by thin-bedded Tertiary carbonates. No diamictite bed is found in Armenia, where the spheroid bed is overlain with a limestone conglomerate containing altered glass shards and shocked quartz. These discoveries indicate that ejecta are emplaced in large terrestrial impacts by at least two distinct flows: (1) an initial flow involving a volatile-rich cloud of fine debris similar to a volcanic pyroclastic flow, which extends >4.7 crater radii (the spheroid bed), and (2) a later flow of coarse debris that may not extend much beyond 3.6 crater radii (the diamictite bed). The former deposit we attribute to material entrained in the impact vapor plume, and the latter to the turbulent collapse of the ejecta curtain.

Keywords: Chicxulub crater, impact ejecta, Cretaceous-Tertiary boundary, Mexico; Belize.

INTRODUCTION

Out-of-crater ejecta deposits from the Chicxulub impact are the best preserved of any large crater on Earth, and they provide an ideal opportunity to study impact processes. The distal, global ejecta deposits from Chicxulub are well known through decades of research related to the Cretaceous-Tertiary (K-T) boundary and mass extinction of life apparently caused by the impact. Studies in northern Belize reveal that a portion of the ejecta blanket is exposed south of the crater (Ocampo et al., 1996; Pope et al., 1999; Smit, 1999; Fouke et al., 2002; King and Petruny, 2003).

In this paper we report on our ongoing study of Chicxulub impact ejecta surface exposures, including new outcrops in southern Quintana Roo, México and central Belize (Fig. 1). These outcrops provide the only known exposures of the outer portion (3.3–4.7 crater radii) of the ejecta blanket from a large impact crater. Impact ejecta deposits in this region comprise the Albion Formation, which is subdivided into two lithostratigraphic sub-units following previous work at Albion Island, Belize (Ocampo et al., 1996; Pope et al., 1999). These two sub-units are named the spheroid bed and diamictite bed, following the common use of the term “bed” to designate small formation sub-units (e.g., Salvador, 1994).

SOUTHERN QUINTANA ROO

Geological maps of México indicate that the Cretaceous is not exposed in the Mexican portion of the Yucatán Peninsula (INEGI, 1987). Nevertheless, our 1997 and 2001 geological reconnaissance along the highway from Ucum to La Unión in southern Quintana Roo, México, discovered several outcrops of Chicxulub impact ejecta and exposures of the underlying Upper Cretaceous Barton Creek Formation (Fig. 2). These new

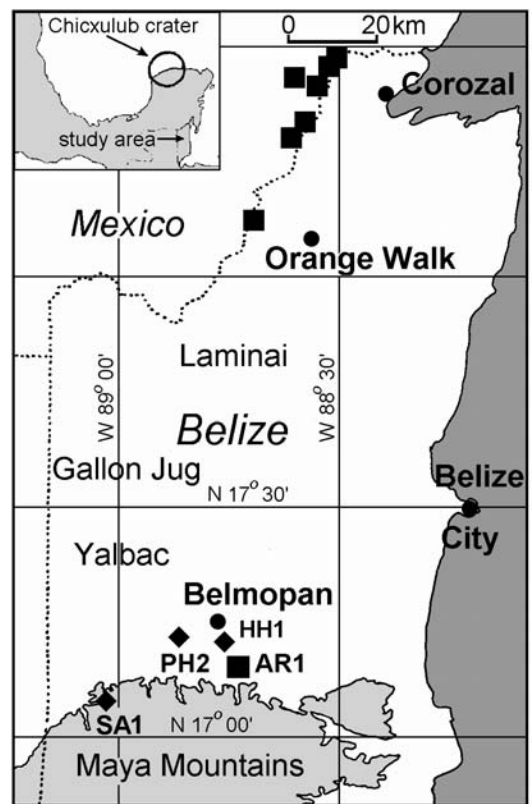


Figure 1. Map of northern Belize and southern Quintana Roo, México, showing Chicxulub impact ejecta outcrops. Square symbols mark location of Albion Formation ejecta outcrops (see Figure 2 for detailed locations of ejecta outcrops along the México-Belize border; not all can be shown at this scale). Diamonds mark other locations mentioned in text. AR1—Armenia 1, PH2—Pook’s Hill 2, SA1—San Antonio 1, and HH1—Hummingbird Highway 1. Lightly shaded region at bottom of map is area above 200 m elevation.

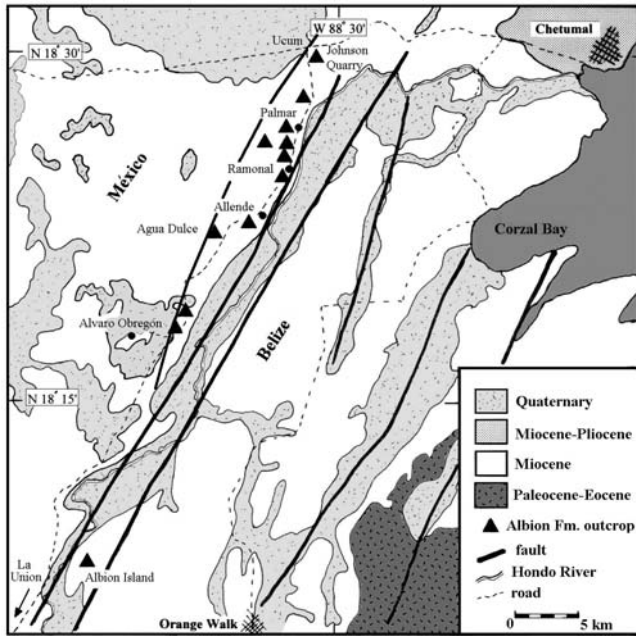


Figure 2. Geological map of southern Quintana Roo, México and northern Belize showing locations of new Albion Formation ejecta outcrops (triangles), as well as the original discovery site at Albion Island (some triangles mark multiple sites, see Appendix for list of outcrop coordinates). Recent research demonstrates that the Upper Cretaceous carbonates are exposed in several areas formerly mapped as Miocene in both México and Belize. Mexican portion of map from Instituto Nacional de Estadística, Geografía, e Informática (INEGI, 1987). Belize portion from Cornec (1986).

ejecta outcrops lie ~330–350 km southeast from the center of the Chicxulub crater. The ejecta deposits belong to the Albion Formation previously identified on Albion Island in nearby northern Belize (Ocampo et al., 1996; Pope et al., 1999). The Albion Formation exposures in Quintana Roo are found in a series of road cuts along the highway that parallels the Río Hondo and in nearby quarries between the towns of Ucum and Alvaro Obregón (Fig. 2). Reconnaissance of road cuts and quarries further south from Alvaro Obregón to La Unión produced no Albion Formation outcrops. Locations of 15 sites with confirmed impact ejecta in this region are given in Appendix 1. The closest site to Chicxulub is the Johnson quarry site (Fig. 2), which contains Albion Formation diamictite deposits 330 km from the center of Chicxulub. The combined Albion Formation exposures in Belize and Quintana Roo indicate that a surface or near-surface discontinuous sheet of impact debris is preserved for ~40 km along the Río Hondo, covering at least a 70 km².

We conducted detailed studies of four locations: Ramonal North, Ramonal South, Agua Dulce, and Alvaro Obregón (Figs. 3–6), which all lie 335–350 km from Chicxulub. The basal contact of the Albion Formation with the underlying Barton Creek Formation is well exposed at Ramonal South (Fig. 3). The only site with an exposed upper contact of the Albion Formation

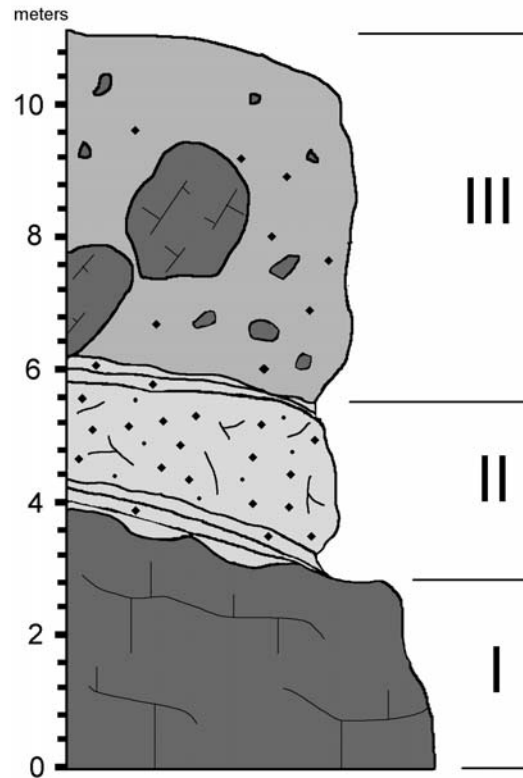


Figure 3. Ramonal South stratigraphic section. (I) Deeply weathered Barton Creek Formation dolomite with iron oxide staining, calcite veins, and abundant solution cavities. (II) 5%–20% green clay clasts 1–20 mm diameter; 5% micritic carbonate clasts including white chalky limestone clasts 5–20 mm diameter with rare clasts up to 4 cm in diameter; rare (~1%) carbonate accretionary lapilli 1–20 mm in diameter; common arcuate fracture planes with thin clay linings. At the base of stratum II are ~1% thin flakes of micritic limestone 1–5 cm in diameter (rip-up clasts?) within multiple layers of orange, purple, and red clay and calcite silts (shear plane?). Similar orange, purple, and red clay and calcite silts in thin layers (shear plane?) at top of unit. (III) 30% micritic limestone and dolomite cobbles and boulders (up to 3 m in diameter) supported in a matrix of calcite and dolomite silt; 10% green clay clasts 1–20 mm in diameter, commonly in lenses.

is Agua Dulce, where the weathered top of the ejecta deposit is overlain by Tertiary limestones (Fig. 6). The other two sites, Ramonal North and Alvaro Obregón, have good exposures of ejecta, but no upper or lower contact.

Ramonal South

Field Observations

The Barton Creek Formation at Ramonal South exhibits extensive karst weathering with local relief of 3–10 m in the surface of a heavily recrystallized limestone with iron-oxide staining, caliche deposits, abundant vugs and travertine deposits. Well-preserved fossils are rare due to the recrystallization, but several Late Cretaceous nerineid gastropods (Pope et al., 1999)

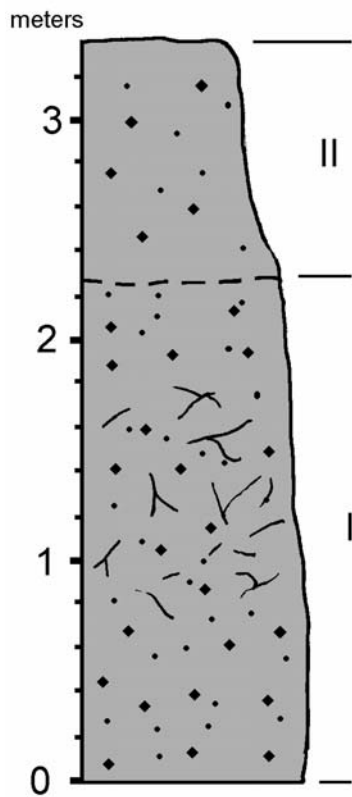


Figure 4. Ramonal North stratigraphic section. (I) 30%–35% green clay clasts 2–40 mm in diameter (mean ~4–6 mm), many clasts have elongated vesicles; 20% carbonate accretionary lapilli 1–25 mm in diameter, most lapilli are coated with red iron oxide and many have cores of limestone and green clay fragments; 1%–3% angular micritic limestone clasts 0.5–5 cm in diameter with rare clasts up to 20 cm; 40% calcite silt matrix; common arcuate fracture planes with thin clay linings. (II) Weathered top of section; 1% green clay clasts 2–20 mm in diameter; 10% carbonate accretionary lapilli 1–25 mm in diameter; 1%–3% angular micritic limestone clasts 0.5–5 cm in diameter; 85% calcite silt matrix; abundant roots.

were found in Barton Creek outcrops between Ramonal South and the town of Allende. This confirms that the Cretaceous is exposed in southern Quintana Roo. Ongoing research in Quintana Roo has recovered a rather diverse Upper Cretaceous fauna in the Barton Creek Formation. Several species of bivalves and gastropods are being studied. A new species of the gastropod *Aporrhais* represents the first record for that genus in the Cretaceous of the Gulf Coast and Caribbean Provinces (Vega et al., 2001). Although the stratigraphic range for this genus extends from Lower Cretaceous to Recent, specimens from Quintana Roo show similarities to species from the Maastrichtian of Montana and Germany.

Overlying the Barton Creek Formation at Ramonal South is a 2-m-thick section of the Albion Formation spheroid bed, which is overlain by a 5-m-thick section of the diamictite bed that extends

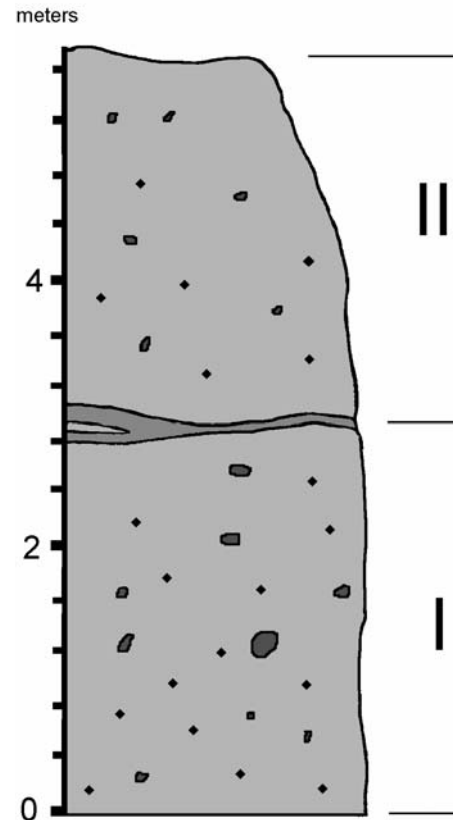


Figure 5. Alvaro Obregón stratigraphic section. (I) 30% sub-angular to sub-rounded micritic dolomite and limestone pebbles and cobbles up to 25 cm in diameter; 10% green clay clasts 3–20 mm in diameter. (II) 20% sub-angular to sub-rounded micritic dolomite and limestone pebbles and cobbles up to 30 cm in diameter; 5% green clay clasts. These two units are separated by a horizontal layer of orange calcitic clay with slickensides (shear plane?).

to the surface (Figs. 3 and 7). The upper and lower contacts of the spheroid bed are marked by 2–20-cm-thick layers of orange, purple, and green calcitic clay with common slickensides. These clay layers appear to be shear planes. There is an abrupt appearance of large micritic dolomite clasts above the upper shear plane and one large dolomite boulder rests immediately on top (Fig. 7). Field tests with HCl indicate that the base of the spheroid bed is calcitic, and becomes progressively more dolomitic near the top. The diamictite bed matrix is dolomitic.

Laboratory Analyses

We examined 12 thin sections from the top of the Barton Creek Formation and from the spheroid and diamictite beds at Ramonal South. Here we describe the textures and key aspects of the mineralogy. Estimates of the percentages (area) of major constituents were made using photomicrographs and percentage charts. The top of the Barton Creek exhibits abundant iron oxide staining, secondary coarse calcite filling fractures and vugs,

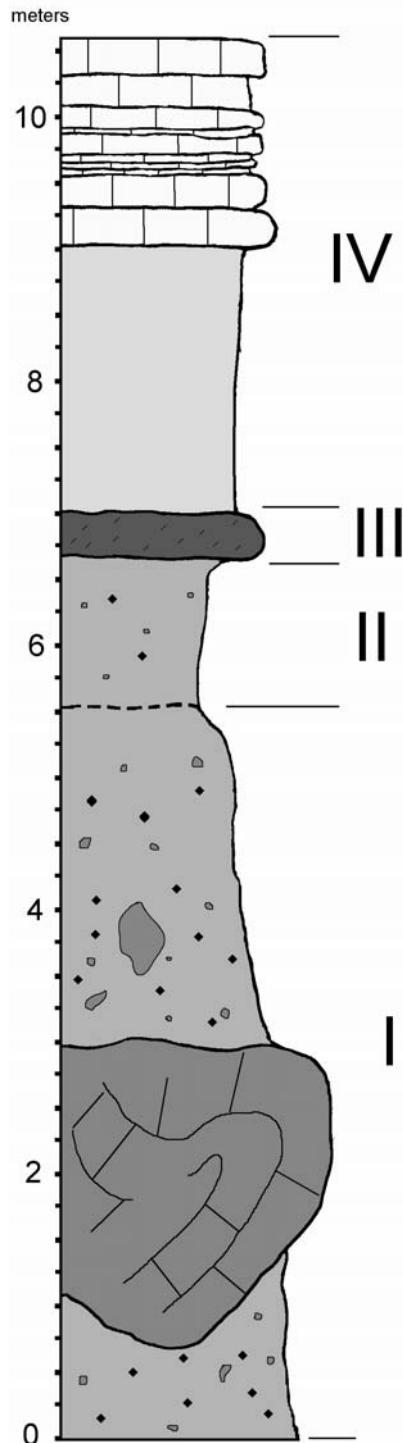


Figure 6. Agua Dulce stratigraphic section. (I) 25% sub-angular to sub-rounded micritic dolomite and limestone pebbles, cobbles, and boulders up to 3.2×9.0 m in size; 5%–10% green clay clasts; fewer (5%) cobbles and boulders in the upper part. (II) 10% micritic dolomite clasts 1–15 cm in diameter; 1%–3% green and orange clay clasts 0.5–2 cm in diameter; 85% matrix of coarse calcite silt with orange and purple iron oxide staining (weathered version of stratum I); (III) calcite cemented caliche with large 2–3 mm calcite crystals; (IV) weathered white micritic dolomite overlying pink and tan, thin-bedded, micritic limestone.

and polycrystalline calcite replacement of dolomite rhombs (de-dolomitization) (Fig. 8), all consistent with a subaerially weathered surface. The main stratum of the spheroid bed (stratum II, Fig. 3) contains 20% yellowish-green clay with spherulitic devitrification features and relict vesicles typical of altered glass (Fig. 9). The spheroid bed contains 20% carbonate clasts of various types, including foraminifera fragments (Fig. 9), and 3% accretionary lapilli (core-type, Schumacher and Schmincke, 1991) composed of aggregates of detrital calcite grains 10–125 μm in size (Figs. 9). The matrix of the spheroid bed is composed of detrital calcite grains similar in size and character to that of the accretionary lapilli aggregates. Some portions of the matrix are altered to interlocking grains of dolomite, especially near the top of the bed. Thin section analysis of the diamictite bed reveals that it is pervasively dolomitized, but contains 10% clay and 20% dolomite clasts (>0.5 mm) of various types (smaller clasts are completely recrystallized) (Fig. 10).

Ramonal North

Field Observations

The Ramonal North road cut exposes a 3.6 m section of the spheroid bed in a dip in Ucum–La Unión highway ~ 200 m north of Ramonal South (Figs. 4 and 11). Neither the top nor the base of the spheroid bed is exposed in the road cut, but the Albion Formation diamictite bed crops out ~ 30 m behind the road cut, suggesting the top of this exposure may be near the upper contact with the diamictite bed. The base of the Ramonal section lies ~ 13 m below the base of the spheroid bed at Ramonal South. We interpret this elevation difference as a dip in the paleo-karst landscape, as the exposed surface of the Barton Creek Formation at Ramonal South is sloping toward Ramonal North and this surface is observed to undulate up and down in numerous road cuts along the Ucum–La Unión highway.

Laboratory Analyses

We analyzed 17 thin sections from the Ramonal North spheroid bed. Yellowish-green clay fragments comprise 20% of the bed and contain common relict vesicles and spherulitic devitrification features typical of altered glass (Figs. 12). No preserved glass was found. Calcite accretionary lapilli of diverse types comprise 10% of the bed, and range in size from 0.2 to 5.0 mm, and average ~ 1.0 mm (Figs. 13–15). There are many examples of what are sometimes classified as mantled lapilli—lithic cores coated with fine ash (Fig. 15), and both rim-type and core-type accretionary lapilli—aggregates of fine detrital grains, with or without a fine-grained rim (Schumacher and Schmincke, 1991). We refer to all types as accretionary lapilli, in part for simplicity, but also because it is not always apparent whether the core is an aggregate or lithic fragment when the latter is rounded and has a similar lithology to the aggregate. Rim-type accretionary lapilli are the most abundant type (Fig. 13), but core-type are also common (Fig. 14), as are ones with limestone (Fig. 15) and clay (altered glass) lithic cores (Fig. 14). The detrital calcite grains in the lapilli aggregates range

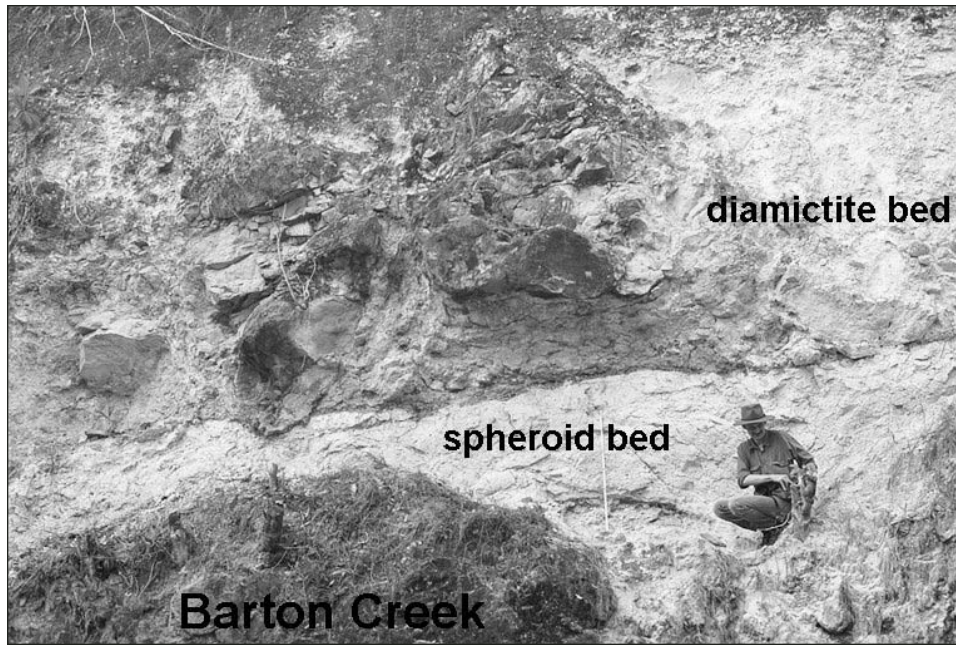


Figure 7. Ramonal South outcrop photograph showing the spheroid bed overlaying the Barton Creek Formation and the diamictite bed overlaying the spheroid bed. Note large boulder resting on contact between spheroid and diamictite beds.

in size from 150 μm to $<10 \mu\text{m}$, and the outermost rims are typically composed of very fine particles ($<10 \mu\text{m}$). Detrital grains are nearly all calcite, but clay fragments (altered glass?) make up 1%–3% of the aggregate. Detrital carbonate clasts ($>100 \mu\text{m}$) of various lithologies, including foraminifera tests (Fig. 14), comprise 5% of the spheroid bed in thin section and occur in approximately the same size range as the accretionary lapilli, although there is no discernable lower size limit (there is a continuum between these clasts and the matrix). The matrix, arbitrarily defined here as that fraction $<100 \mu\text{m}$, comprises ~60%–70% of the thin sections and is composed mostly of detrital carbonate grains and a few percent clay. The matrix and the lapilli aggregate are essentially the same composition.

Two samples of the clay (altered glass fragments) from within the spheroid bed were analyzed by X-ray diffraction after air drying, glycolation, and heating to 550 $^{\circ}\text{C}$, using a Philips PW1710 X-ray diffractometer at the Geological Survey of Canada. Both were found to be smectite with traces of mixed layer smectite-illite.

Alvaro Obregón

Field Observations

The road cut at Alvaro Obregón exposes 7.5 m of the diamictite bed (Fig. 5) separated by a sub-horizontal (dips slightly south) orange calcitic clay layer a few centimeters thick with slickensides on the upper and lower surfaces. This clay layer is positioned ~2.6 m up from the base of the exposure and extends the length (~100 m) of the road cut (Fig. 16). As at Ramonal South, we interpret this clay layer as a shear plane. Rare cobbles in the diamictite bed have striated surfaces, polish, and accretionary rinds. There is no upper or lower diamictite bed contact

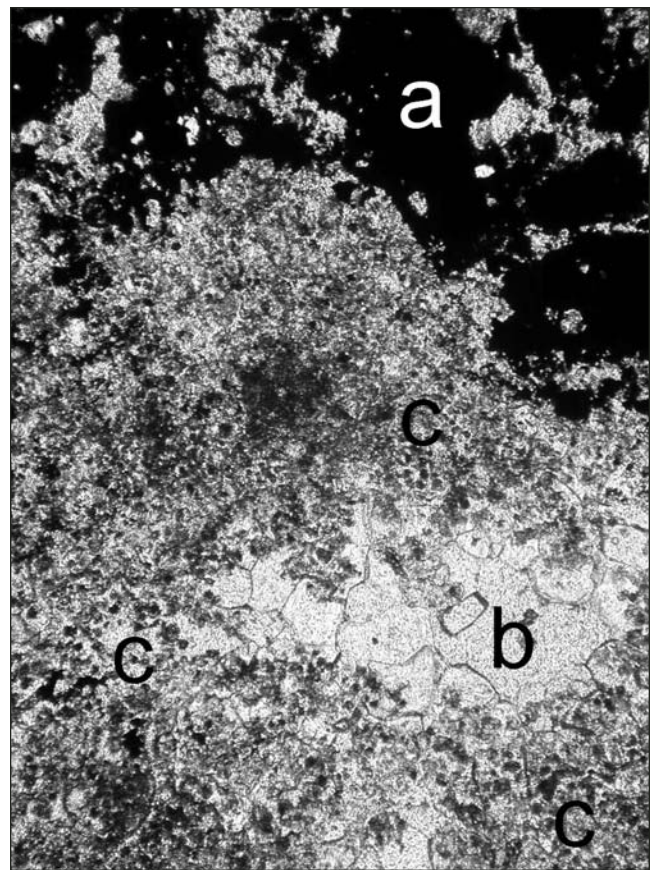


Figure 8. Photomicrograph of thin section from the upper contact of the Barton Creek Formation at Ramonal South showing (a) iron oxide staining; (b) secondary coarse calcite filling cavities; and (c) polycrystalline calcite (light) replacing dolomite (dark cores). Plane polarized transmitted light. Field of view: 2.8 mm wide.

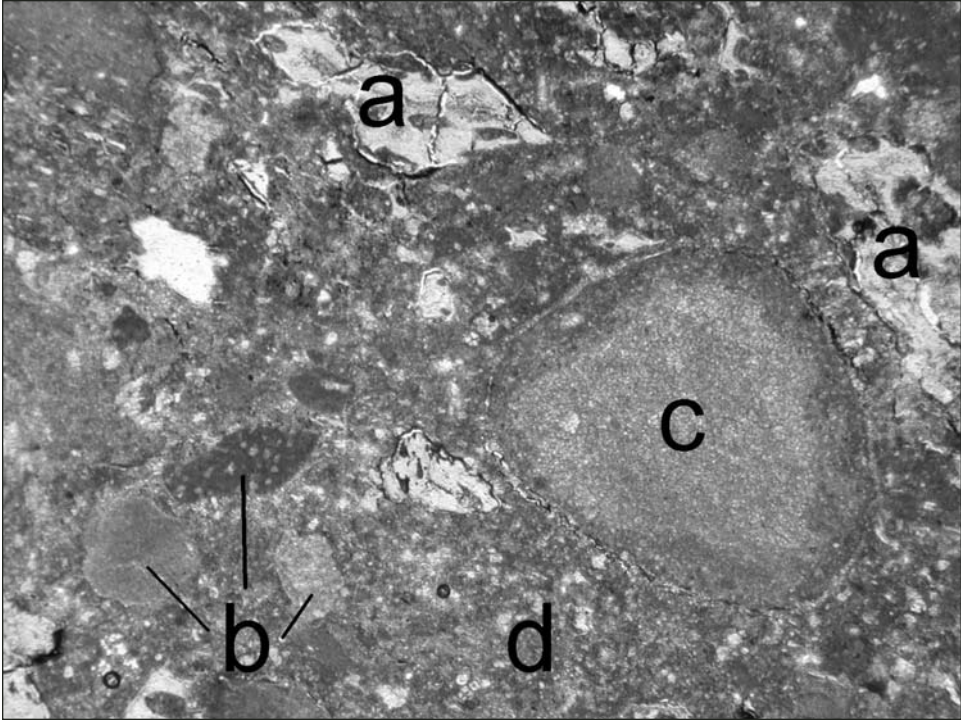


Figure 9. Photomicrograph of thin section from the Ramonal South spheroid bed showing (a) clay fragments with elongated vesicles filled with carbonate matrix; (b) micritic limestone clasts (center arrow foraminifera); (c) accretionary lapilli; (d) matrix of detrital carbonate grains. Plane polarized transmitted light. Field of view: 4.4 mm wide.

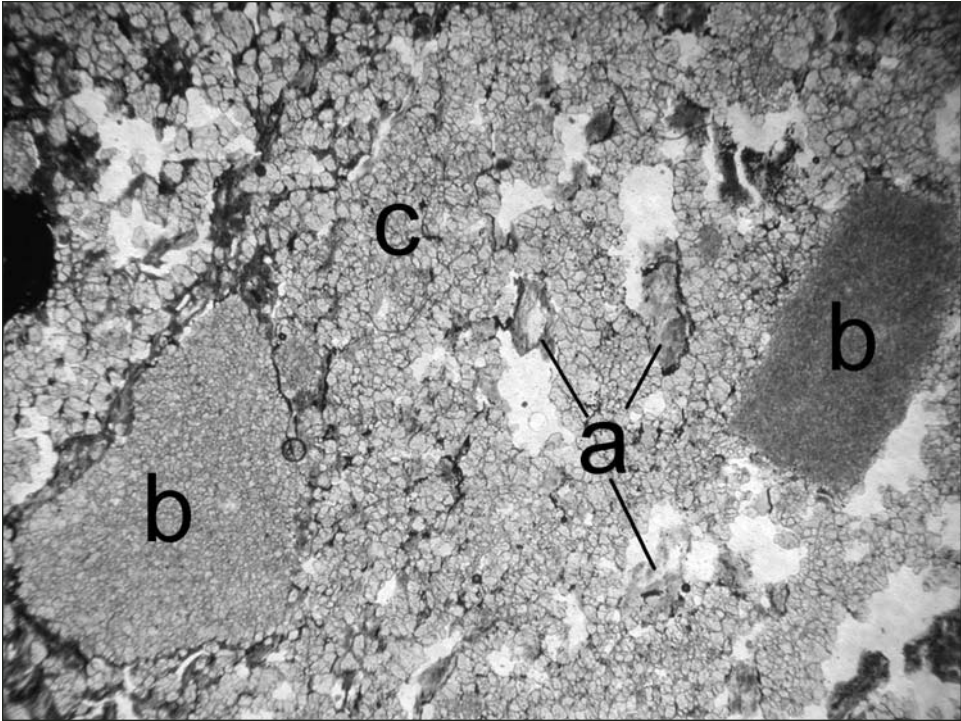


Figure 10. Photomicrograph of thin section from the base of the diamictite bed Ramonal South showing (a) clay fragments; (b) recrystallized coarse grain dolomite (left) and fine grained limestone (right) clasts; and (c) coarse grained dolomite matrix (recrystallized). Plane polarized transmitted light. Field of view: 6.0 mm wide.

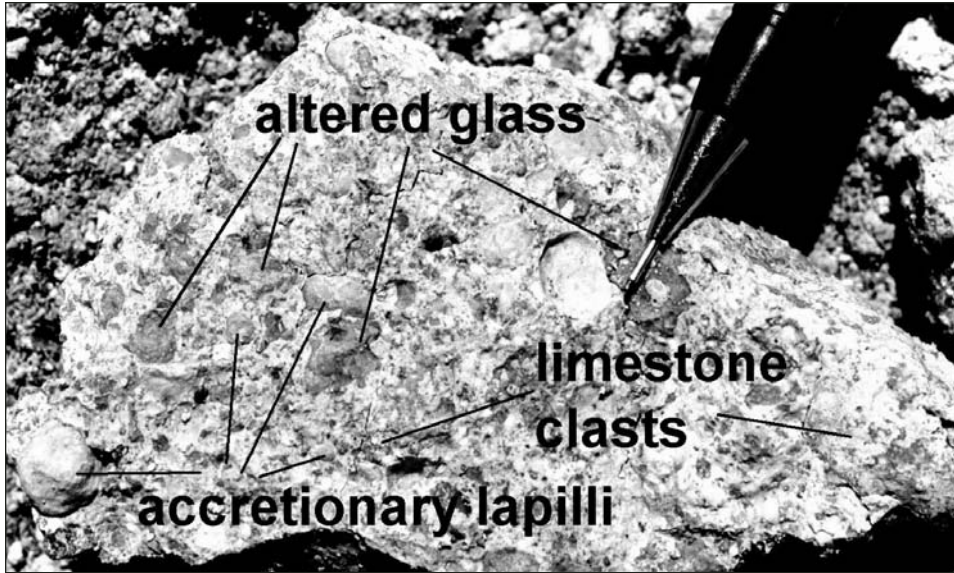


Figure 11. Hand sample of Ramonal North spheroid bed showing abundant accretionary lapilli and clay fragments (altered glass) and common limestone clasts.

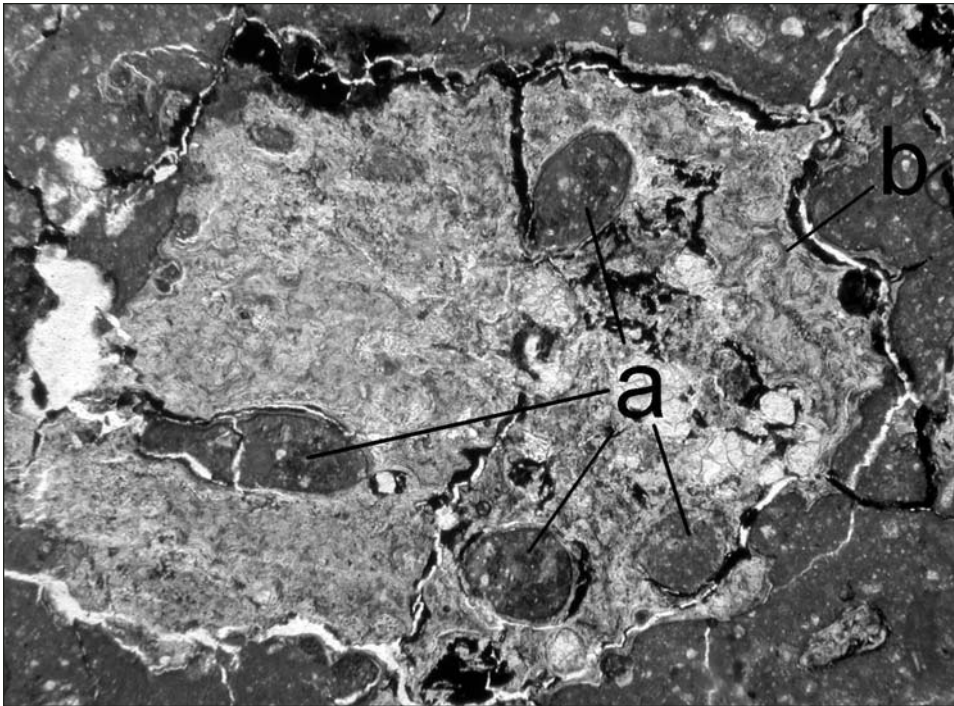


Figure 12. Photomicrograph of thin section from the Ramonal North spheroid bed showing a large clay fragments with (a) elongated vesicles filled with carbonate matrix; and (b) spherulitic devitrification features. Plane polarized transmitted light. Field of view: 4.2 mm wide.

exposed at Alvaro Obregón. Tests with dilute HCl indicate that the upper stratum is mostly dolomitized, whereas the base is only partially dolomitized and contains several micritic limestone clasts 1–20 cm in diameter and a slightly calcitic matrix.

Laboratory Analyses

We analyzed seven thin sections from the Alvaro Obregón diamictite bed. The bed contains 10% yellowish-green clay fragments, which like those in the spheroid bed, possess relict

vesicles and spherulitic devitrification features typical of altered glass (Fig. 17). Angular to sub-rounded carbonate clasts $>100\ \mu\text{m}$ in size comprise 25% of the thin sections, some of which retain poorly preserved foraminifera (Fig. 18). Most carbonates are recrystallized to dolomite, which makes it difficult to discern clast boundaries for the smaller clasts as they merge with the 10–40 μm recrystallized dolomite matrix. The predominant clast lithology is a light brown dolomite with $\sim 20\text{--}40\text{-}\mu\text{m}$ -sized interlocking dolomite crystals and indistinct clast-matrix boundaries (Fig. 18).

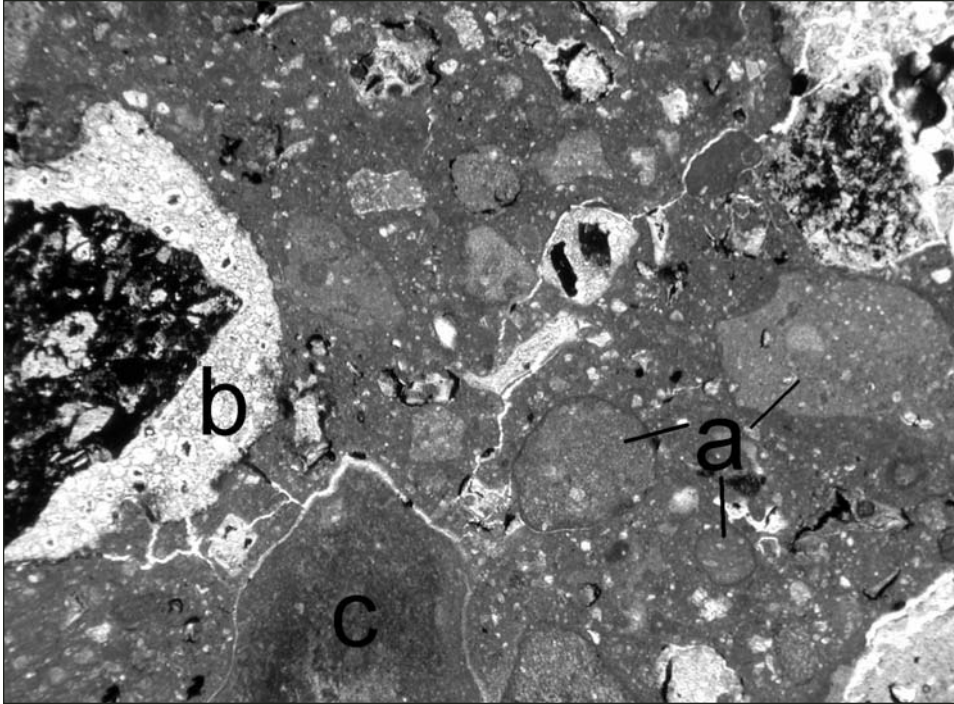


Figure 13. Photomicrograph of thin section from the Ramonal North spheroid bed showing (a) accretionary lapilli composed of coarse carbonate detrital grains with a very thin, fine (<10 μm) accretionary rim (rim-type); (b) lithic clast with a spherulitic altered glass rim; and (c) angular limestone clast. Plane polarized transmitted light. Field of view: 5.9 mm wide.

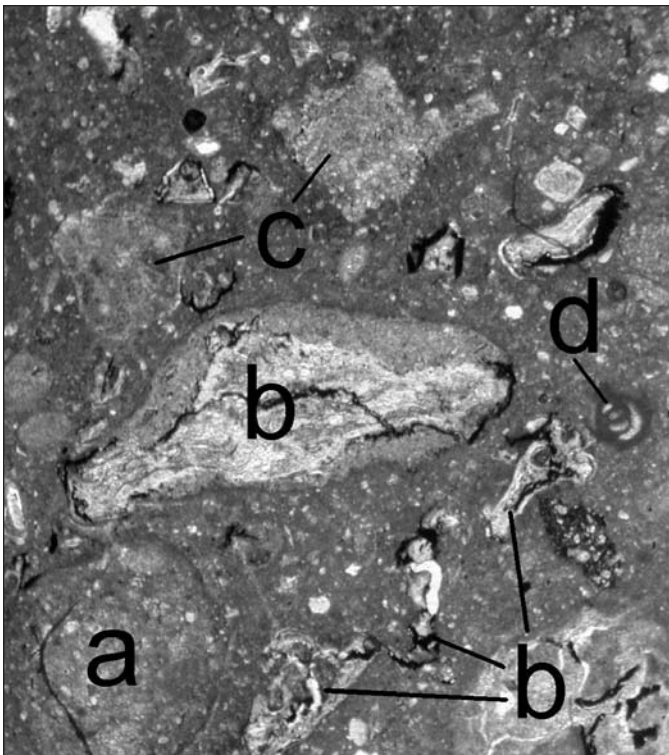


Figure 14. Photomicrograph of thin section from the Ramonal North spheroid bed showing (a) accretionary lapilli composed of coarse carbonate detrital grains (core type); (b) clay clasts with relict vesicles and flow banding (center), note altered glass fragment with accretionary rind (center); (c) carbonate clasts; and (d) foraminifera test. Plane polarized transmitted light. Field of view: 3.0 mm wide.

Agua Dulce

Field Observations

The road cut at Agua Dulce extends for ~500 m and exposes an 8-m-thick sequence of the diamictite bed (Fig. 6) with many large micritic dolomite boulders (Fig. 19). The diamictite bed here is similar to that found at Alvaro Obregón, except for the abundance of large boulders (compare the photos in Figs. 16 and 19). Tests with dilute HCl indicate that the diamictite bed clasts and matrix at Agua Dulce are only partially dolomitized. The Agua Dulce section contains one very large dolomite boulder (9.0 \times 3.2 m) that has highly deformed bedding (Fig. 19). The upper (~2 m) part of the diamictite bed has fewer large cobbles and clay clasts, but the change is gradational. The top ~1 m of the diamictite bed is a weathered horizon capped with well-indurated caliche. Overlying this caliche are over 10 m of thin-bedded dolomite and limestone.

Laboratory Analyses

We analyzed seven thin sections from the Agua Dulce diamictite bed. The bed contains 15% yellowish-green clay fragments with the same relict vesicles and spherulitic devitrification features indicative of altered glass found at Alvaro Obregón (Fig. 20). Angular to sub-rounded carbonate clasts >100 μm in size comprise 25% of the thin sections, some with preserved foraminifera (Fig. 20). Some carbonate clasts are recrystallized to dolomite, and the previously noted clasts of light brown dolomite with 20–40 μm -sized interlocking dolomite crystals and indistinct clast boundaries are present (Fig. 20). Dolomite clasts

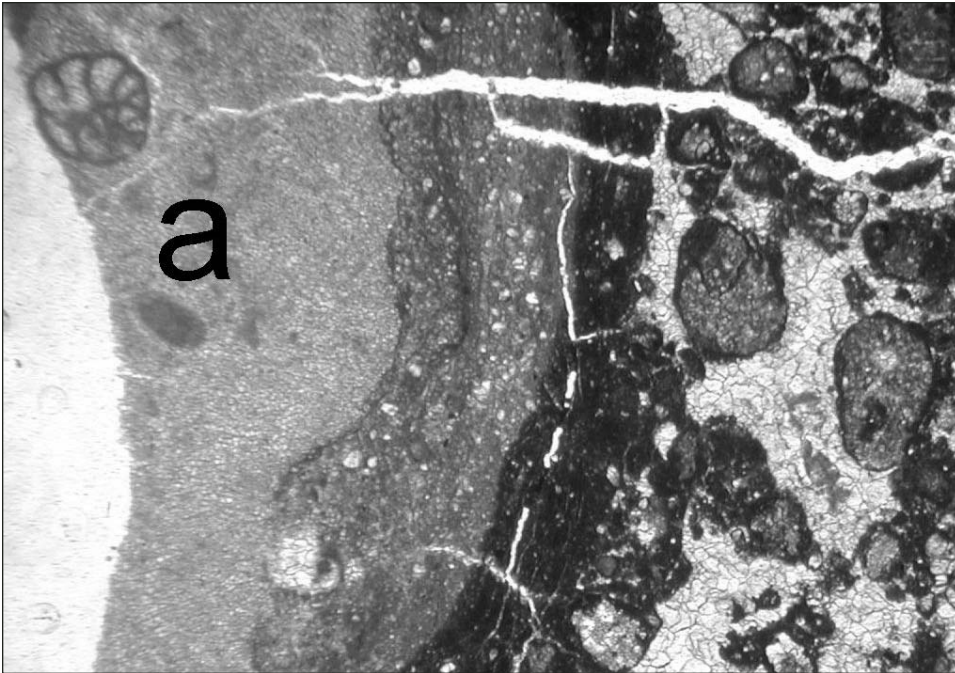


Figure 15. Photomicrograph of thin section from the Ramonal North spheroid bed showing a large accretionary lapilli with (a) a micritic limestone lithic core with a foraminifera test that is encased by multiple layers of accreted detrital calcite grains. Outer dark color is due to iron oxide staining of outer layers. Plane polarized transmitted light. Field of view: 4.3 mm wide.



Figure 16. Alvaro Obregón road cut exposing Albion Formation diamictite bed. Note horizontal calcitic clay layer (shear plane?) along the center of the outcrop. Exposure is 7.5 m high.

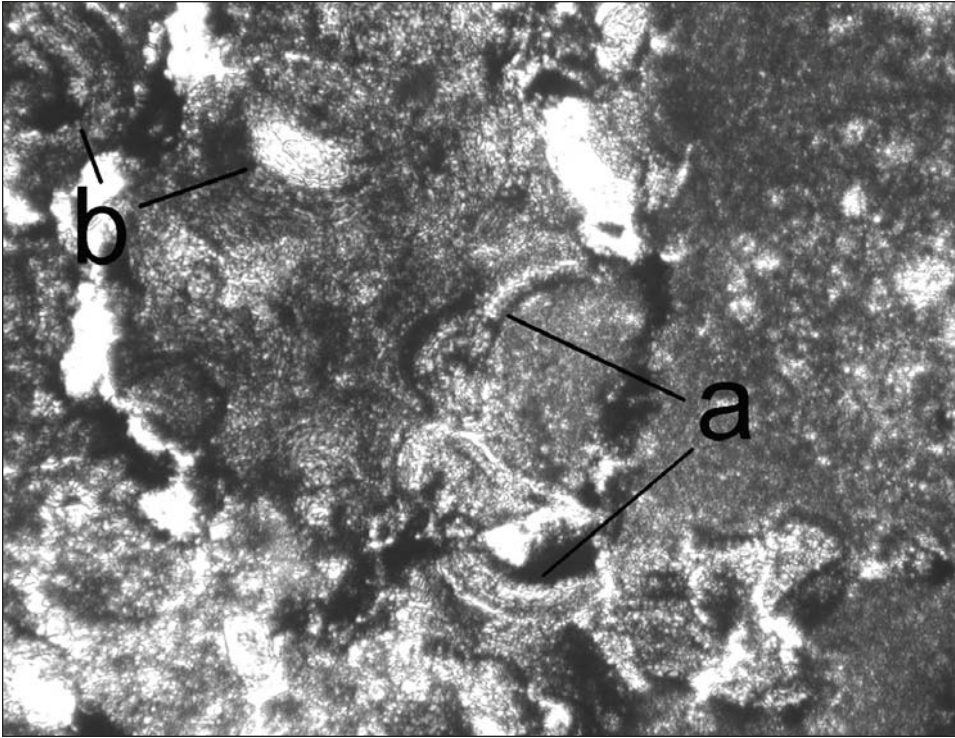


Figure 17. Photomicrograph of thin section from near the base of the Alvaro Obregón diamictite bed showing a clay fragment (altered glass) with (a) relict vesicles filled with matrix and (b) spherulitic devitrification features. Plane polarized transmitted light. Field of view: 1.9 mm wide.

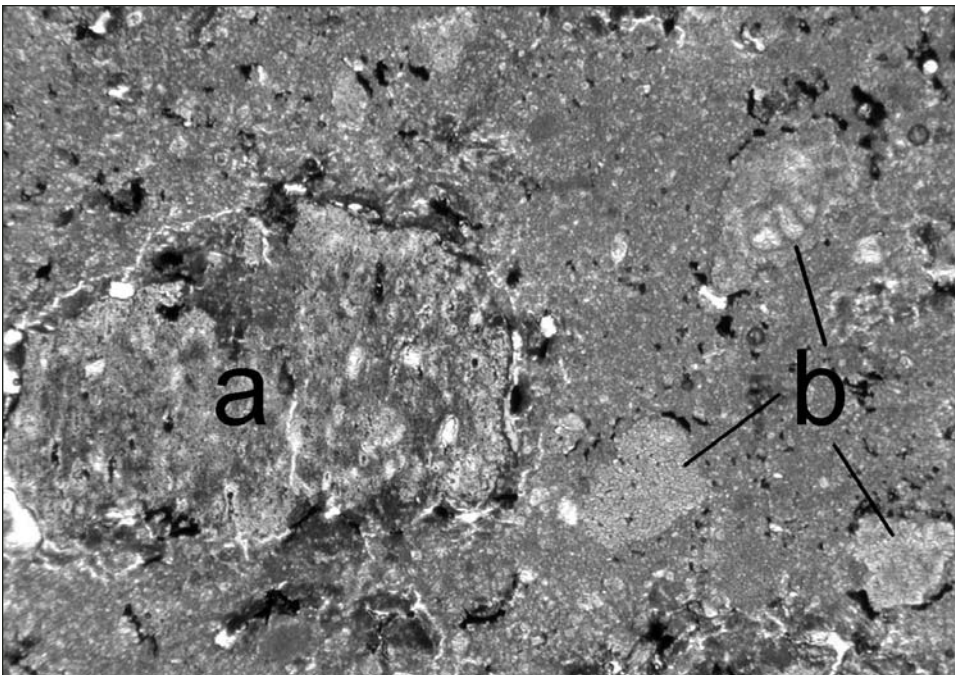


Figure 18. Photomicrograph of thin section from near the base of the Alvaro Obregón diamictite bed showing (a) a clay fragment (altered glass) with elongated vesicles; and (b) lithic clasts of coarse dolomite, one with a foraminifera test, in a mostly fine grained calcite and dolomite matrix. Field of view: 4.2 mm wide.

are not as abundant as at Alvaro Obregón, and micritic limestone clasts are common. The carbonate matrix is finer-grained at Agua Dulce (less altered) than at Alvaro Obregón, and small clast boundaries are more distinct.

Four clay separates (altered glass fragments) were analyzed by X-ray diffraction and are dominated by smectite with traces of mixed layered smectite-illite.

NORTH-CENTRAL BELIZE

The discovery of Chicxulub impact ejecta along the Belize-México border prompted our search for more distal ejecta deposits further south, in Belize. The preservation of Chicxulub ejecta on Albion Island, an uplifted block of Cretaceous carbonate platform sediments associated with the Río Hondo fault zone (Ocampo et al., 1996; Pope et al., 1999), suggests that other juxtaposed fault-blocks of Cretaceous and Tertiary platform carbonates in north-central Belize may preserve remnants of Chicxulub ejecta. Nevertheless, our reconnaissance of Cretaceous blocks near Gallon Jug, Laminai, and Yalbac (Fig. 1) produced no evidence of impact ejecta. Thus, if Chicxulub ejecta deposits existed in this region, they have apparently been stripped by erosion.

Late Cretaceous and early Tertiary platform carbonates are well known in central Belize (Ower, 1928; Dixon, 1956; Flores 1952a, 1952b; Cornec, 1985; King et al., 2004). Marine sedimentation is thought to be discontinuous across the K-T boundary (Flores, 1952b), but the stratigraphic relationship between Cretaceous and Tertiary strata in Belize has not been studied in much detail. Upper Cretaceous Barton Creek Formation outcrops with rudist fragments were identified by Flores (1952a, 1952b) along the base of the Maya Mountains (Fig. 1). Paleocene sediments have not been previously identified in this region, but outcrops of shallow marine Paleocene carbonates are found 35 km northeast of Belmopan (Flores 1952a, 1952b). Lower Eocene limestones outcrops of the El Cayo Group are common along the northern flanks of the Maya Mountains (Flores 1952a, 1952b). A major uplift of the Maya Mountains began in the early Tertiary involving the reactivation of the northern boundary fault of the Maya Mountains (Fig. 1) (Bateson and Hall, 1977).

We examined stratigraphic sections along the northern flanks of the Maya Mountains in the vicinity of juxtaposed Cretaceous and Tertiary blocks shown on the geologic map of Belize (Cornec, 1986). The complex tectonism and the thick tropical vegetation made it difficult to trace contacts between sections. The upper contact of the Barton Creek Formation in this region is a highly irregular karst surface with relief of 10–30 m and exposures of caves and rubble-filled solution cavities. The Barton Creek carbonates near the upper contact are a coarse, recrystallized limestone with abundant calcite-filled fractures and vugs, but grade down-section into dolomitized limestones. Good exposures of the weathered top of the Barton Creek are found at Pook's Hill 2 (PH2), Hummingbird Highway 1 (HH1), and San Antonio 1 (SA1) (Fig. 1). At 15 locations we found the Barton Creek Formation overlain by 10–30 m of pebbles, cobbles, and

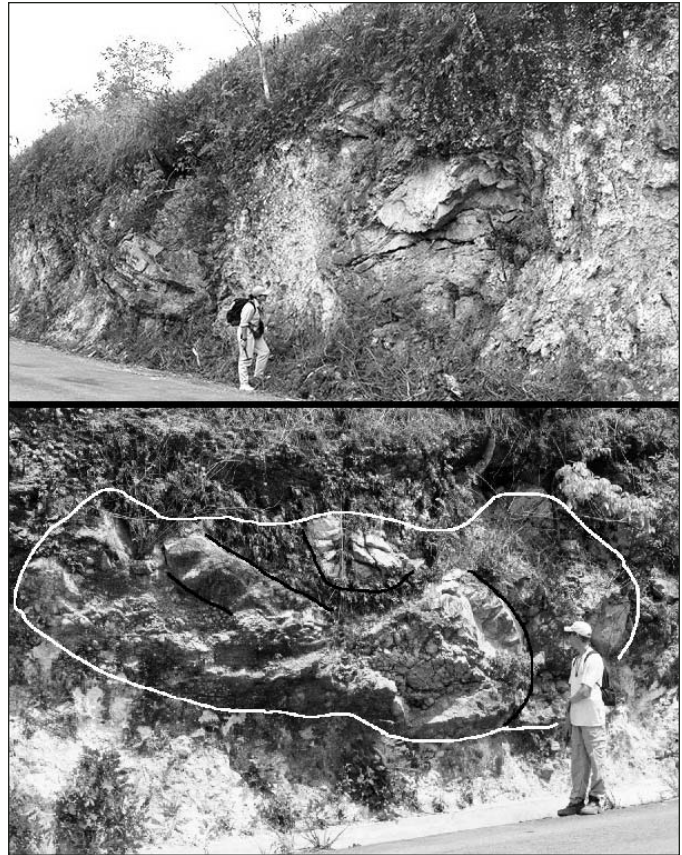


Figure 19. Agua Dulce road cut with large dolomite boulders in the Albion Formation diamictite bed. All have major axis roughly parallel to the ground surface. Upper two boulders both ~6–7 m long, lower one is 9 m (outline in white, black lines mark extreme folding in relict beds).

boulders supported in a matrix of red clay and coarse calcite silt. The coarse size fraction (>1 cm) of this unit is a mixture of angular to rounded clasts, but sub-rounded clasts dominate. Clast sizes range from sub-millimeter grains to 2 m diameter boulders, but most clasts are <30 cm in diameter. The clast lithology is a diverse mixture of carbonates, including micritic limestone, coarse crystalline limestone, laminated dolomite, breccia, and calcareous mudstone. The coarse crystalline limestone is the most common lithology, and is probably derived from the weathered Barton Creek Formation. We interpret this unit as a regolith or saprolite resulting from the karst weathering of the Barton Creek Formation, but we recognize that its genesis may well be complex and not solely the product of in situ weathering given the diverse clast lithologies.

Tertiary sediments overly the Barton Creek regolith at Pook's Hill 2 (PH2, Fig. 1), but the contact is not well exposed and is marked by an abrupt change in the lithology of clasts eroding out of the bulldozed upper slopes of a hill. These Tertiary sediments are a cream-colored fossiliferous dolomite with abundant rocky-shore bivalves and gastropods, including *Mytilus*

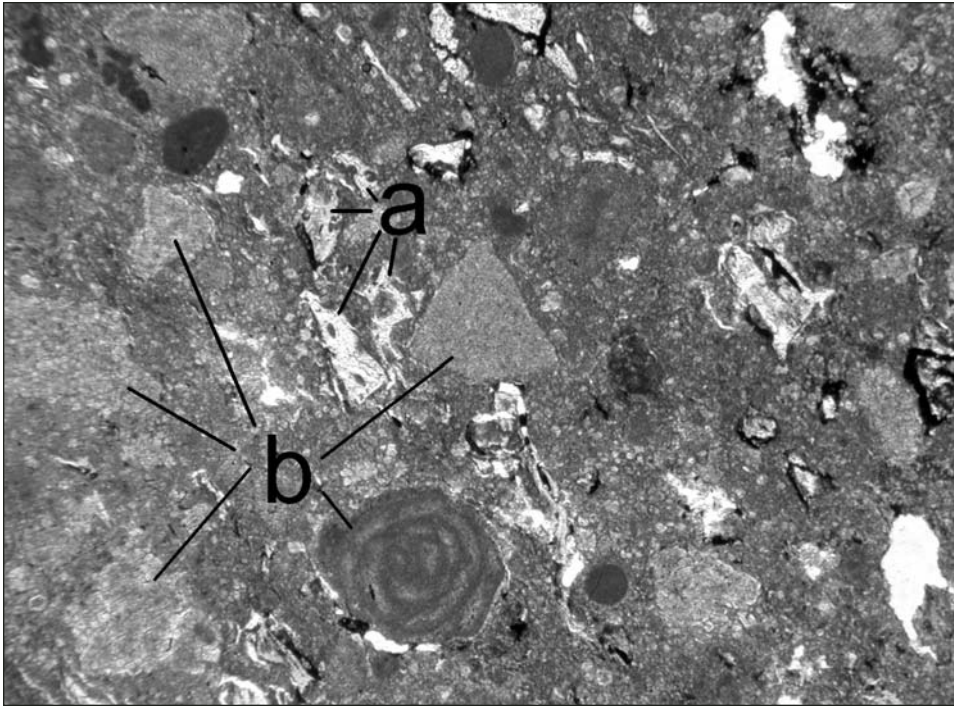


Figure 20. Photomicrograph of thin section from middle of the Agua Dulce diamictite bed showing (a) clay fragments (altered glass) with matrix filled vesicles; and (b) lithic clasts of coarse dolomite with indistinct boundaries (grains on left) and micritic limestone (grains on right), one with a foraminifera test, in a mostly fine grained calcite and dolomite matrix. Plane polarized transmitted light. Field of view: 5.1 mm wide.

sp., *Septifer* sp., and *Puncturella* sp. This fauna marks the beginning of the Tertiary marine transgression on the edge of the Maya Mountains, and a similar assemblage is typical of Paleocene transgression sequences in the southern United States (e.g., Palmer and Palmer, 1937).

We conclude that, as at Albion Island and Ramonal South, the northern flanks of the Maya Mountains were uplifted and subjected to karst weathering at the end of the Cretaceous. This finding suggests that remnants of Chicxulub ejecta may be found associated with the regolith that caps this weathered surface. Thus far our research has confirmed Chicxulub ejecta associated with this regolith cap at only one location, near the village of Armenia, 470 km from Chicxulub.

Armenia

Field Observations

Near the village of Armenia we found a 5-m-thick exposure of the Albion Formation spheroid bed overlying the terminal Cretaceous regolith in a road cut along the Hummingbird Highway south of Belmopan (Figs. 1, 21, and 22). The spheroid bed contains abundant, angular green and red altered glass fragments and accretionary lapilli in a calcite silt matrix (Fig. 23). Underlying the spheroid bed is 50–150-cm-thick stratum of calcitic red clay with weathered limestone cobbles overlying an ~5-m-thick indurated regolith deposit. The highly oxidized state (deep red color), clay texture, and prismatic structure of the calcitic red clay stratum suggest that it is a paleosol. Deeply weathered Barton Creek Formation exposures occurs in road cuts just north of Armenia,

but at Armenia the base of the regolith is a shear zone, perhaps formed by the collapse of a solution cavity or by a fault. Overlying the spheroid bed is an ~5-m-thick matrix supported limestone pebble and cobble conglomerate (Fig. 22).

Laboratory Analyses

We analyzed 10 thin sections from the Armenia spheroid bed and underlying clay stratum. Analyses of the calcitic red clay of the paleosol shows that it contains 10% small rounded limestone clasts 0.2–3 mm in diameter and lenticular clay clasts in sharp contact with the overlying spheroid bed (Fig. 24). Analyses of samples from the Armenia spheroid bed reveal well-preserved primary textures of the accretionary lapilli and clay clasts similar to those found at Ramonal North. Greenish and reddish brown clay fragments comprise ~20% of the bed and contain common relict vesicles and spherulitic devitrification features typical of altered glass (Figs. 25). Portions of the larger altered glass fragments are translucent, lack devitrification features, have patches that are nearly isotropic, and thus are probably palagonite, an early alteration product of glass.

Calcite accretionary lapilli of diverse types comprise 20% of the spheroid bed in thin section, range in size from 0.3 to 5.0 mm, and average 1.0 mm (Fig. 25). Rim-type, core-type, and ones with lithic cores are all common, but as at Ramonal North, rim-type accretionary lapilli predominate. The detrital calcite grains that comprise the accretionary lapilli range in size from ~140 μm to <10 μm . Clay fragments comprise <1% of the lapilli aggregate, but angular clay lithic cores, some with relict vesicles, are common (Fig. 23). Detrital micritic limestone clasts (>100



Figure 21. Armenia road cut showing Albion Formation spheroid bed resting on deeply weathered Upper Cretaceous Barton Creek Formation. Just below the spheroid bed is a dark red calcitic clay interpreted as a terminal Cretaceous paleosol. Overlying the spheroid bed are 5 m of limestone conglomerate.

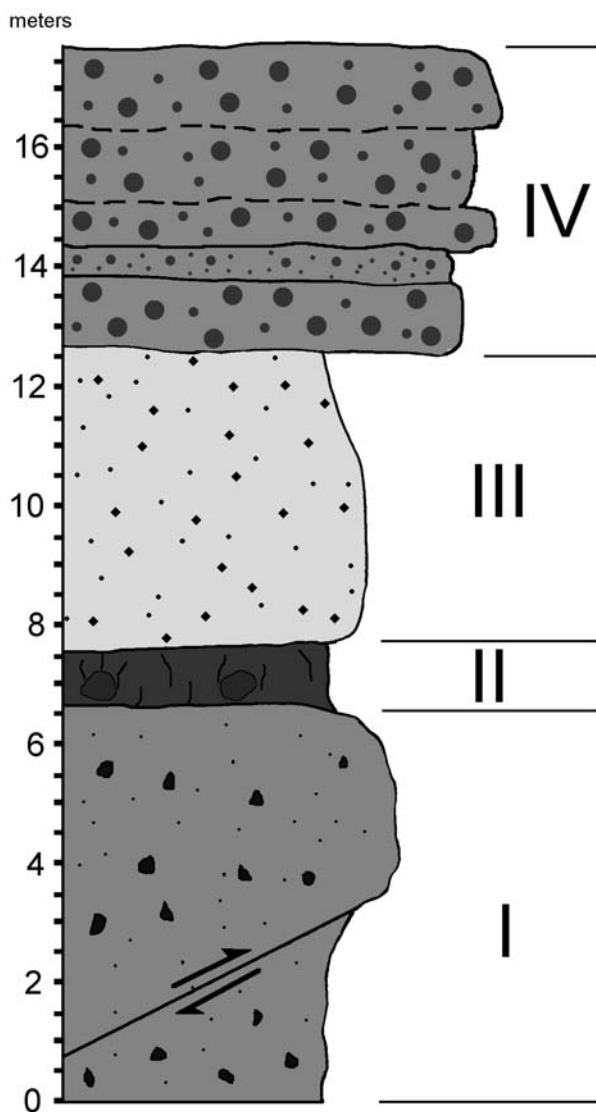


Figure 22. Armenia stratigraphic section. (I) 20% sub-rounded to angular micritic limestone and dolomite pebbles and cobbles supported in a red calcitic clay matrix; abundant secondary calcite in fractures and cavities. This stratum is in fault contact with a breccia unit with similar clasts and matrix, but includes large blocks of the overlying strata. (II) dark red calcitic red clay with 10% small rounded and angular pebbles and grains 1–5 mm. There are several large (10–30 cm) deeply weathered cobbles and a faint prismatic soil structure. (III) 20%–30% green clay clasts, many with vesicles; 10%–20% calcite accretionary lapilli 1–60 mm in diameter, (mean 5 mm), most larger (>0.5 cm) lapilli have cores of limestone or clay clasts; 1%–3% micritic limestone clasts 10–80 mm in diameter (mean 12 mm). (IV) 60%–75% sub-rounded micritic limestone, rare chert and dolomite, pebbles and cobbles 1–50 cm in diameter (mean ~5–10 cm); many cobbles exhibit a fine polish, striations, gouges, penetrating grains, and hinge fractures; 25%–40% matrix of sand and silt-sized limestone and clay clasts rarely occurring as sandy lenses; the stratum is weakly consolidated, but there are several layers that are cemented with calcite cement.



Figure 23. Hand sample of Armenia spheroid bed showing abundant accretionary lapilli and clay fragments (altered glass)—dark fragments in light colored detrital calcite matrix. Note that the large accretionary lapilli has a core of clay (altered glass, dark in photo).

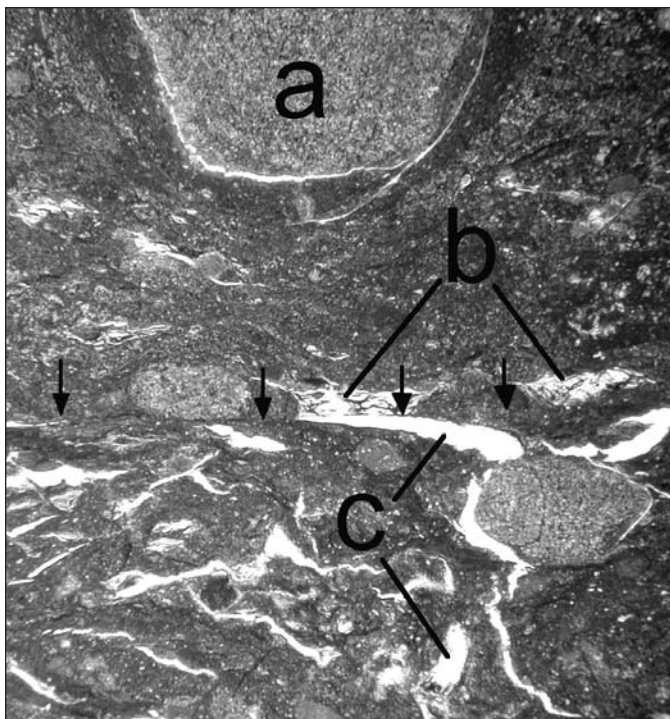


Figure 24. Photomicrograph of thin section of the basal contact of the Armenia spheroid bed showing a sharp contact (arrows) and (a) abrupt appearance of accretionary lapilli; (b) translucent clay clasts (altered glass; note minor mixing [one rounded limestone grain resting above contact]); (c) root casts, some with intact roots, probably modern. Plane polarized transmitted light. Field of view: 4.4 mm wide.

μm) comprise 5% of the spheroid bed in thin section. About 50%–60% of the spheroid bed is a fine-grained calcite matrix with essentially the same composition and size distribution as the accretionary lapilli aggregate.

One clay sample (altered glass fragment) from the Armenia spheroid bed was analyzed with X-ray diffraction and found to be predominately an interstratified mixed layer illite-smectite with a large portion composed of illite.

We examined 15 slides with grain residues prepared from acid leached samples of the Armenia spheroid bed matrix. Residues were mounted in oil, which allows the grains to be rotated to view all axes, but not to measure the angle. We found no shocked quartz in the spheroid bed (detrital quartz was quite rare in these samples). We also examined 10 slides with grain residues prepared in the same fashion from samples of the matrix of the conglomerate bed that immediately overlies the Armenia spheroid bed. We found nine detrital quartz grains with multiple sets (8 with 2 sets, 1 with 3 sets) of planar deformation features (PDFs) indicative of impact shock (Figs. 26A–26C), and several more with a single set of PDFs. We calculate that there are ~4 grains with multiple PDFs per gram of matrix. Vesicular glass shards (50–500 μm), now altered to clay, are also a common conglomerate matrix constituent at Armenia (Fig. 26D). The relatively abundant shocked quartz in the conglomerate bed is unlikely reworked from the spheroid bed, as the latter lacks shocked quartz. Presumably, the conglomerate contains ejecta reworked from another source, or is itself an impact deposit. Further research is needed to test these two possibilities.

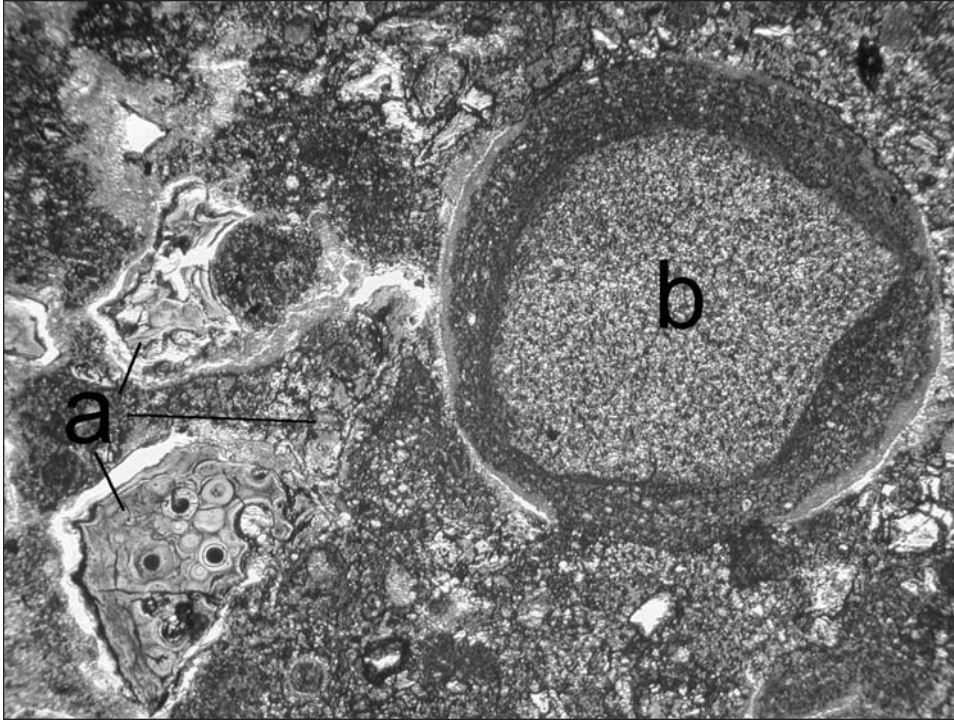


Figure 25. Photomicrograph of thin section from the lower portion of the Armenia spheroid bed showing (a) clay clasts with matrix filled vesicles and spherulitic devitrification features and (b) rim-type accretionary lapilli. Plane polarized transmitted light. Field of view: 2.7 mm wide.

COMPARISONS WITH OTHER EJECTA DEPOSITS

The new Albion Formation outcrops in Quintana Roo and central Belize show close similarities with those from Albion Island and help confirm that Chicxulub ejecta are exposed over a broad area at the base of the Yucatán Peninsula. Our interpretation that these deposits are impact ejecta is based primarily upon the occurrence of abundant altered vesicular glass fragments and carbonate accretionary lapilli, which cannot be explained by any known volcanic activity in the region. Their association with the Chicxulub impact is established by the large thickness and dominant carbonate lithology, which are appropriate for the nearby Chicxulub crater, and by their stratigraphic position resting on a terminal Cretaceous land surface. These criteria are critical, since carbonate breccias are common near the K-T boundary in this region. These new sites also help confirm a regional subdivision of the Albion Formation, originally proposed from Albion Island (Ocampo et al., 1996), into a basal spheroid bed and overlying diamictite bed. The thickest deposit remains the one at Albion Island, where recent (2001) quarrying has exposed a 17-m-thick section.

An important aspect of the new outcrops is that they are much less altered than those on Albion Island and thus better preserve primary textures and mineralogies. The Albion Formation matrix, clasts, and accretionary lapilli on Albion Island are all pervasively dolomitized (Ocampo et al., 1996; Pope et al., 1999; Fouke et al., 2002). The better preserved spheroid bed outcrops at Ramonal North and Armenia confirm that the original carbonate mineralogy

of this unit was calcite, and that the carbonate “spheroids” are, without a doubt, accretionary lapilli analogous to ones found in volcanic pyroclastic deposits. Similarly, the altered glass fragments with vesicular textures are much better preserved at Ramonal North and Armenia than in the spheroid bed at Albion Island, although it appears that little to no true glass remains. The diamictite bed at Alvaro Obregón and Agua Dulce is also slightly less dolomitized than its equivalent at Albion Island, and we speculate that the matrix of this unit was also originally calcite. Likewise, it is clear that the diamictite bed contains both limestone and dolomite clasts, but their original abundances are difficult to determine given the pervasive postdepositional dolomitization.

The only other reported Chicxulub ejecta deposit with a discrete bed of accretionary lapilli is at Guayal, in Tabasco, México, located ~550 km southwest from the center of Chicxulub (Grajales-Nishimura et al., 2000; Salge et al., 2000). While the texture of the Guayal lapilli is similar to those of the Albion Formation spheroid bed at Ramonal North and Armenia, the composition is very different. The Guayal lapilli contain shocked quartz grains (Grajales-Nishimura et al., 2000) and are reported to be 64% quartz, 19% clay, 9% calcite, and 8% dolomite (Salge et al., 2000), but much of this quartz may be secondary (Griscom et al., 1999). This abundance of quartz and paucity of calcite, if primary, is in marked contrast to the Albion Formation spheroid bed. It should be noted that the Guayal lapilli bed was deposited in deep water, contains many fragmented lapilli, and is associated with a massive slump of debris triggered by the impact, and thus it may not be a primary deposit. No accretionary lapilli beds have been reported

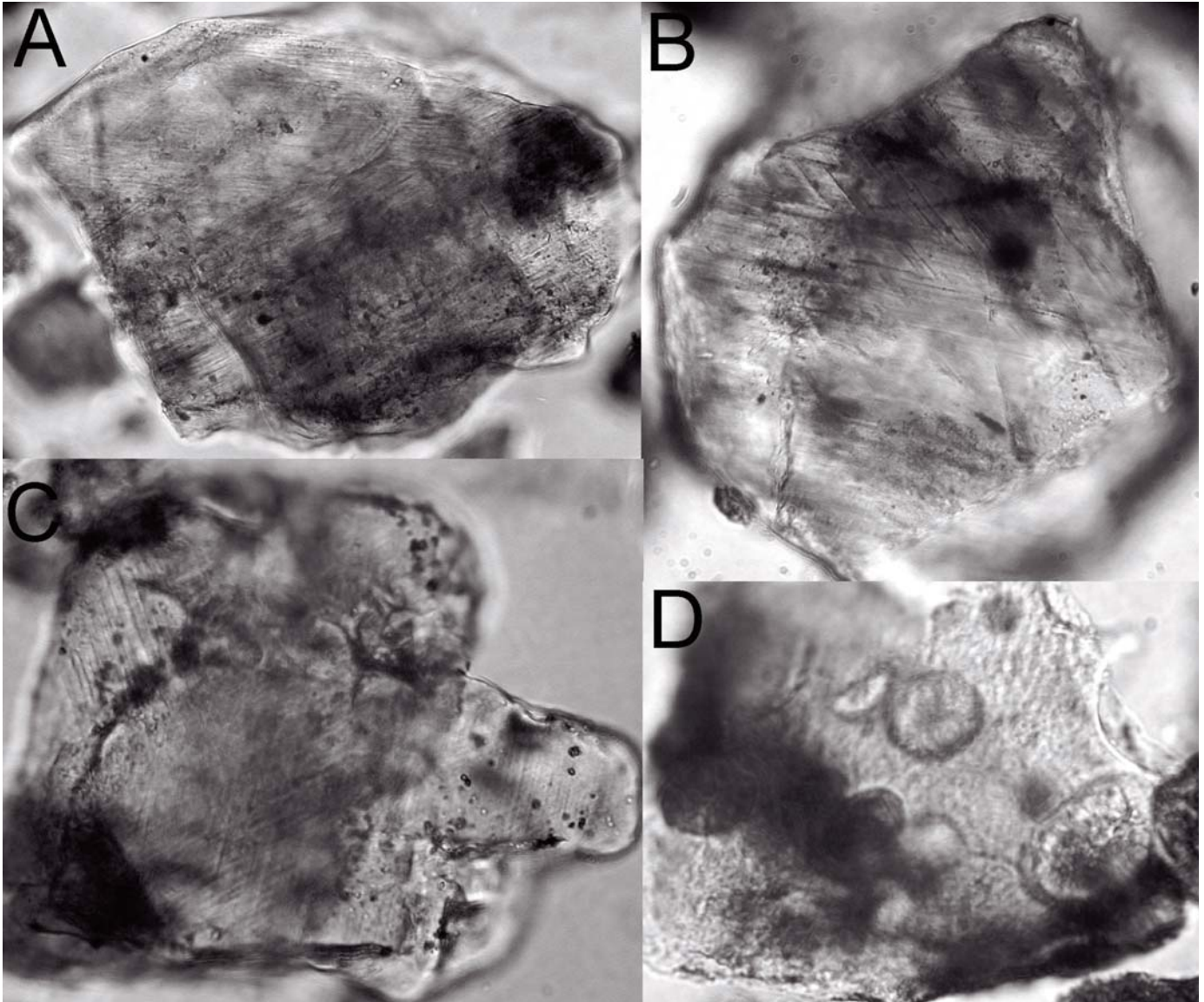


Figure 26. (A–C) Detrital shocked quartz grains with multiple sets of planar deformation features (PDFs). (D) Altered glass shard with vesicles and spherulitic devitrification features, all from the matrix of the limestone conglomerate bed overlying the Armenia spheroid bed. All grains mounted in oil and shown in plane polarized transmitted light. (A) 240 μm , 2 sets PDFs; (B) 215 μm , 2 sets PDFs; (C) 140 μm , 3 sets PDFs; (D) 160 μm .

from deposits closer to the Chicxulub crater, in ejecta deposits drilled by Universidad Nacional Autónoma de México (UNAM) and Petróleos Mexicanos (Pemex) (Sharpton et al., 1996; Corrigan, 1998), or by the Intercontinental Drilling Program (ICDP) (Dressler et al., 2003). Our own examination of the UNAM cores in 2003 likewise found no accretionary lapilli. Calcite accretionary lapilli are found in Chicxulub ejecta deposits at sites more distal than Guayal in northeastern México (Smit et al., 1996), but these lapilli are apparently rare and do not form discrete beds.

Accretionary lapilli have been reported from the crater-fill suevite of several other impact craters, for example Ries (Graup, 1981), Sudbury (Muir and Peredery, 1984), Manson (Witzke and

Anderson, 1996), and Popigai (Masaitis, 2003). No accretionary lapilli occur in the out-of-crater ejecta at Ries. Carbonate lapilli similar to those in the Albion Formation occur in discrete beds in the Alamo breccia impact deposits in Nevada, which, like Chicxulub, is interpreted as a carbonate platform impact (Warne et al., 2002). Nevertheless, these lapilli beds are more like the one at Guayal, as they have been redeposited by high-energy submarine flows, and their exact location with respect to the impact site is not known.

None of these other impact accretionary lapilli deposits provide a good analogue for the Albion Formation spheroid bed, and the best comparison is with volcanic pyroclastic deposits.

Massive deposits of mixed mantled, core, and rim-type accretionary lapilli, which characterize the Albion Formation spheroid bed, have their closest analogues with ash-rich pyroclastic flows or surges produced by large phreatomagmatic eruptions (e.g., Schumacher and Schmincke, 1991). The main contrast is that large phreatomagmatic volcanic eruptions do not typically produce both abundant silicate glass and calcite ash, yet an impact into a mixed silicate-carbonate target would.

The Albion Formation diamictite bed is similar to, yet distinct from, the more proximal ejecta deposits cored near the Chicxulub rim by UNAM and Pemex (e.g., Sharpton et al., 1996, 1999; Corrigan, 1998). These more proximal deposits are divided into two units: (1) a basal polymict breccia called Bunte-type breccias (after the Bunte Breccia of the Ries crater, e.g., Hörz et al., 1983), which contains ~40%–60% sulfate, ~30%–40% carbonate, and <1%–4% silicate basement; and (2) an upper suevitic breccia (a name also derived from Ries) containing 40%–60% silicate basement (Sharpton et al., 1996, 1999). The Chicxulub suevitic breccia extends ~140 km from the crater's center (Sharpton et al., 1999), while the Chicxulub Bunte-type breccia extends more than 200 km (Sharpton et al., 1996). The Albion Formation diamictite bed, while technically classified as a suevitic breccia (mixture of melted and unmelted clasts), contains far less silicate material than is found in the Chicxulub suevitic breccias near the rim, and considerably more melt than is found in the Chicxulub Bunte-type breccia. Furthermore, the 40%–60% sulfate component of the Chicxulub Bunte-type breccia is mostly missing in the diamictite bed, although it is possible that the sulfate once present has been leached.

There are no ejecta blanket deposits from other terrestrial impact craters that are directly comparable to the Albion Formation. The ejecta from the Ries crater, which possesses one of the best studied examples of a terrestrial ejecta blanket, are not preserved beyond 3 crater radii, whereas the Albion Formation outcrops described in this paper extend from 3.3 to 4.7 crater radii. It should also be added that Chicxulub is much larger than Ries (200 km versus 26 km diameter).

The diamictite bed contains <<1% unmelted deep target material (only traces have been found; Ocampo et al., 1996; Pope et al., 1999), and some unknown percentage of shallow target carbonate primary ejecta. This aspect matches well with the studies of Ries, where the Bunte Breccia contains <1% deep target and ~34% shallow target material (Hörz et al., 1983). The main contrast is that the diamictite bed contains 10% shock-melted deep target material (the altered glass), which is absent in the Ries Bunte Breccia. Another contrast between the diamictite bed and the Ries Bunte Breccia is that there is little evidence of erosion at the base the Albion Formation diamictite bed, given the intact spheroid bed at all three basal exposures. The emplacement of the Bunte Breccia apparently eroded over 50 m of basal Tertiary unconsolidated sands (Hörz et al., 1977). The Albion Formation diamictite bed is best described as a mixture of the Bunte-type and suevitic breccias, this fact, the lack of erosion at the base, and the deposition of pyroclastic-like flows (the spher-

oid bed) all indicate that ejecta from large craters are emplaced at distances greater than 3 radii by processes somewhat different from those proposed for Ries crater (e.g., Hörz et al., 1983). We suggest that at these greater distances there is more mixing of ejecta, less influence of secondary cratering, and emplacement is by less erosive surface flows.

CONCLUSIONS

We have presented evidence that Chicxulub impact ejecta are preserved in numerous locations in Quintana Roo, México and Belize, at distances of 330–470 km from the center of Chicxulub. It can be debated whether or not thick deposits of the Albion Formation ejecta once ringed the Chicxulub crater and thus formed part of the “continuous ejecta” as seen in images of other terrestrial planets and defined at Ries crater (e.g., Hörz et al., 1983). Thick ejecta deposits have only been found close to the rim and south of Chicxulub (UNAM and Pemex cores, Albion Formation), and this is the only area where typical ejecta blanket deposits are expected, as this region had the only dry land at the time of impact. All other proximal ejecta were emplaced in deep water (e.g., Smit, 1999). We argue that the Albion Formation diamictite bed is part of the Chicxulub continuous ejecta, given its extent (>70 km²) and thickness (>17 m). It is less clear that the Albion Formation spheroid bed should be considered part of the continuous ejecta where it occurs without the overlying diamictite bed, since there is only one site, Armenia, with this stratigraphy. No Albion Formation diamictite bed deposits have been found at distances greater than 3.6 crater radii (Albion Island), and we propose that this may be the approximate limit for the Chicxulub continuous ejecta. We speculate that the abundance of debris along the Río Hondo may represent the terrestrial equivalent of a terminal thickened rampart, as seen along the outer edge of fluidized ejecta blankets on Mars (e.g., Carr et al., 1977).

The discovery of Albion Formation spheroid bed deposits at a distance of 4.7 crater radii (Armenia) demonstrates that this unit was significantly more extensive than the diamictite bed. The limestone cobble bed with shocked quartz and altered impact glass overlying the spheroid bed at Armenia may be impact related, or contain reworked ejecta; research is ongoing to determine which scenario applies. The limited number of spheroid bed outcrops—four, with the most distal one, Armenia, >100 km from the others—precludes any definitive discussion of the distribution of this unit, but some conclusions are warranted. First, we observed no significant differences in thickness, texture, or composition between Ramonal North and Armenia. This apparent homogeneity across >100 km suggests that the ash cloud that produced this accretionary lapilli bed was immense and that the flow evolved little over this distance. Applying a simple energy line model developed for large pyroclastic flows (Sheridan, 1979), suggests that the ash cloud that produced pyroclastic flows at distances of 500 km reached an elevation of ~100 km, not unreasonable for a large impact. The abundance of shock-melted basement (20%–30% altered glass) in deposits

470 km from the impact center is perhaps best explained by the explosive dispersal of shock melt by volatile expansion (Kieffer and Simonds, 1980). The occurrence of this glass with accretionary lapilli, which form in water-rich, ash-laden clouds, indicates that the first and fastest ejecta to leave the crater may have been from massive steam explosions that produced gas-rich, pyroclastic-like flows (Wohletz and Sheridan, 1983).

In summary, we propose that the Albion Formation spheroid bed is a product of explosive vapor plume expansion that dispersed a large volume of shock melt. The vapor was water-rich and upon expansion, condensed to help form the large mass of accretionary lapilli, which were deposited in a mode similar to pyroclastic flows. We interpret the diamictite bed to be derived from the turbulent mixing and collapse of the main ejecta curtain, which moved as a surface flow over the vapor plume deposits until halting somewhere near the current México and Belize border.

ACKNOWLEDGMENTS

This work was supported by the National Aeronautics and Space Administration Exobiology Program, California Institute of Technology, Jet Propulsion Laboratory, The Planetary Society and Belize expedition participants, Natural History Museum of Los Angeles County, and the European Space Agency. We also acknowledge the kind support of the Belizean Geology and Petroleum Office and Pook's Hill Lodge.

APPENDIX

Locations of Albion Formation Outcrops

- (1) Albion Island N18° 07.84' W88° 41.13'
Belize
- (2) Armenia N17° 08.93' W88° 44.07'
Belize
- (3) Johnson Quarry N18° 29.73' W88° 30.89'
México
- (4) Sacxán N18° 27.96' W88° 31.23'
México
- (5) Palmar 1 N18° 27.15' W88° 31.67'
México
- (6) Palmar 2 N18° 26.93' W88° 32.17'
México
- (7) Palmar 3 N18° 26.85' W88° 33.49'
México
- (8) Palmar 4 N18° 26.68' W88° 32.47'
México
- (9) Palmar 5 N18° 26.38' W88° 31.85'
México
- (10) Ramonal North N18° 26.01' W88° 31.90'
México
- (11) Ramonal South N18° 25.71' W88° 31.96'
México
- (12) Allende 1 N18° 22.94' W88° 33.95'
México
- (13) Allende 2 N18° 22.83' W88° 34.27'
México
- (14) Allende 3 N18° 22.52' W88° 34.82'
México

- (15) Sabidos N18° 20.47' W88° 36.33'
México
- (16) Agua Dulce N18° 20.16' W88° 36.66'
México
- (17) Alvaro Obregón N18° 17.88' W88° 37.185'
México

REFERENCES CITED

- Bateson, J.H., and Hall, I.H.S., 1977, The geology of the Maya Mountains: Institute of Geological Studies, Natural Environmental Research Council, Overseas Memoir, v. 3, p. 1–38.
- Carr, M.H., Crumpler, L.S., Cutts, J.A., Greeley, J.E., Guest, J.E., and Masursky, H., 1977, Martian impact craters and emplacement of ejecta by surface flows: *Journal of Geophysical Research*, v. 82, p. 4055–4065.
- Cornec, J.H., 1985, Note on the Provisional Geological Map of Belize at the scale of 1:250,000: Petroleum Office, Ministry of Natural Resources, Belmopan, Belize, p. 22.
- Cornec, J.H., 1986, Geological Map of Belize: Geology and Petroleum Office, Ministry of Natural Resources, Belmopan, Belize, scale 1:250,000.
- Corrigan, C.M., 1998, The Composition of Impact Breccias from the Chicxulub Impact Crater, Yucatan Peninsula, Yucatan, Mexico [M.S. thesis]: East Lansing, Michigan State University, p. 125.
- Dixon, C.G., 1956, Geology of Southern British Honduras: Belize City, Belize Government Printer, p. 92.
- Dressler, B.O., Sharpton, V.L., and Marin, L.E., 2003, Chicxulub YAX-1 impact breccias: Whence they come? [abs.]: Lunar and Planetary Institute, Houston, Texas, USA, *Lunar and Planetary Science*, v. 34, abstract no. 1259 (CD-ROM).
- Flores, G., 1952a, Geology of northern British Honduras: American Association of Petroleum Geologists Bulletin, v. 36, p. 404–409.
- Flores, G., 1952b, Summary Report of the Preliminary Geological Studies of the area N of 17° N Latitude, British Honduras: Freeport, Bahamas Exploration Company, LTD, 35 p.
- Fouke, B.W., Zerkle, A.L., Alvarez, W., Pope, K.O., Ocampo, A.C., Wachtman, R.J., Grajales-Nishimura, J.M., Claeys, P., and Fischer, A.G., 2002, Cathodoluminescence petrography and isotope geochemistry of KT impact ejecta deposited 360 km from the Chicxulub crater, at Albion Island, Belize: *Sedimentology*, v. 49, p. 117–138, doi: 10.1046/j.1365-3091.2002.00435.x.
- Grajales-Nishimura, J.M., Cedillo-Pardo, E., Rosales-Domínguez, C., Padilla-Avila, P., Sánchez-Ríos, A., Morán-Zenteno, D.J., Alvarez, W., Claeys, P., Ruiz-Morales, J., and García-Hernández, J., 2000, Chicxulub impact: The origin of reservoir and seal facies in the southeastern Mexico oil fields: *Geology*, v. 28, p. 307–310, doi: 10.1130/0091-7613(2000)0282.3.CO;2.
- Graup, G., 1981, Terrestrial chondrules, glass spherules and accretionary lapilli from the suevite, Ries crater, Germany: *Earth and Planetary Science Letters*, v. 55, p. 407–418, doi: 10.1016/0012-821X(81)90168-0.
- Griscom, D.L., Beltran-Lopez, V., Merzbacher, C.I., and Bolden, E., 1999, Electron spin resonance of 65-million-year-old glasses and rocks from the Cretaceous-Tertiary boundary: *Journal of Non-Crystalline Solids*, v. 253, p. 1–22, doi: 10.1016/S0022-3093(99)00340-3.
- Hörz, F., Gall, H., Hüttner, R., and Oberbeck, V.R., 1977, Shallow drilling in the Bunte Breccia deposits, Ries Crater, Germany, *in* Roddy, D.J., Pepin, R.O., and Merrill, R.B., eds., *Impact and Explosion Cratering*: New York, Pergamon, p. 425–488.
- Hörz, F., Ostertag, R., and Rainey, D.A., 1983, Bunte Breccia of the Ries: Continuous deposits of large impact craters: *Reviews of Geophysics and Space Physics*, v. 21, p. 1667–1725.
- INEGI (Instituto Nacional de Estadística, Geografía, e Informática), 1987, Carta Geológica, Chetumal Sheet, Mexico 1:250,000, 1 sheet.
- Kieffer, S.W., and Simonds, C.H., 1980, The role of volatiles and lithology in the impact cratering process: *Review of Geophysics and Space Physics*, v. 18, p. 143–181.
- King, D.T., Jr., and Petruny, L.W., 2003, Stratigraphy and sedimentology of coarse diamictite breccia beds within the Cretaceous-Tertiary boundary section, Albion Island, Belize, *in* Koeberl, C., and Martínez-Ruiz, F., eds., *Impact Markers in the Stratigraphic Record*: Berlin, Springer-Verlag, p. 203–227.

- King, D.T., Jr., Pope, K.O., and Petruny, L.W., 2004, Stratigraphy of Belize, north of the 17th parallel: Transactions of the Gulf Coast Association of Geological Societies, v. 54, p. 289–304.
- Masaitis, V.L., 2003, Obscure-bedded ejecta facies from the Popigai impact structure, Siberia: Lithological features and mode of origin, *in* Koeberl, C., and Martinez-Ruiz, F., eds., Impact Markers in the Stratigraphic Record: Berlin, Springer-Verlag, p. 137–162.
- Muir, T.L., and Peredery, W.V., 1984, The Onaping Formation, *in* Pye, E.G., Naldrett, A.J., and Giblin, P.E., eds., The Geology and Ore Deposits of the Sudbury Structure: Geological Survey of Ontario, p. 139–204.
- Ocampo, A.C., Pope, K.O., and Fischer, A.G., 1996, Ejecta blanket deposits of the Chicxulub crater from Albion Island, Belize, *in* Ryder, G., Fastovsky, D., and Gartner, S., eds., The Cretaceous-Tertiary Event and Other Catastrophes in Earth History: Geological Society of America Special Paper 307, p. 75–88.
- Ower, L., 1928, Geology of British Honduras: Journal of Geology, v. 36, p. 494–509.
- Palmer, K. van W., 1937, The Claibornian Scaphopoda, Gastropoda and Dibrachiate Cephalopoda of the Southern United States: Bulletin of American Paleontology, v. 7, p. 1–730.
- Pope, K.O., Ocampo, A.C., Fischer, A.G., Alvarez, W., Fouke, B.W., Webber, C.L., Jr., Vega, F.J., Smit, J., Fritsche, A.E., and Claeys, Ph., 1999, Chicxulub impact ejecta from Albion Island, Belize: Earth and Planetary Science Letters, v. 170, p. 351–364, doi: 10.1016/S0012-821X(99)00123-5.
- Salge, T., Tagle, R., and Claeys, P., 2000, Accretionary lapilli from the KT boundary site of Guayal, Mexico: Preliminary insights of expansion plume formation: Abstracts of the 63rd Annual Meteoritical Society Meeting, Chicago, Illinois, Abstract 5124.
- Salvador, A., ed., 1994, International Stratigraphic Guide, 2nd ed: International Union of Geological Sciences and Geological Society of America, 214 p.
- Schumacher, R., and Schmincke, H.-U., 1991, Internal structure and occurrence of accretionary lapilli—A case study at Laacher See Volcano: Bulletin of Volcanology, v. 53, p. 612–634.
- Sharpton, V.L., Marin, L.E., Carney, J.L., Lee, S., Ryder, G., Schuraytz, B.C., Sikora, P., and Spudis, P.D., 1996, A model of the Chicxulub impact basin based on evaluation of geophysical data, well logs, and drill core samples, *in* Ryder, G., Fastovsky, D., and Gartner, S., eds., The Cretaceous-Tertiary Event and Other Catastrophes in Earth History: Geological Society of America Special Paper 307, p. 55–74.
- Sharpton, V.L., Corrigan, C.M., Marin, L.E., Urrutia-Fucugauchi, J., and Vogel, T.A., 1999, Characterization of impact breccias from the Chicxulub impact basin: Implications for excavation and ejecta emplacement [abs.]: Houston, Texas, USA, Lunar and Planetary Institute, Lunar and Planetary Science, v. 30, abstract no. 1515 (CD-ROM).
- Sheridan, M.F., 1979, Emplacement of pyroclastic flows: A review, *in* Chapin, C.E., and Elston, W.E., eds., Ash-Flow Tuffs: Geological Society of America Special Paper 180, p. 125–136.
- Smit, J., 1999, The global stratigraphy of the Cretaceous-Tertiary boundary impact ejecta: Annual Reviews of Earth and Planetary Science, v. 27, p. 75–113, doi: 10.1146/annurev.earth.27.1.75.
- Smit, J., Roep, T.B., Alvarez, W., Montanari, A., Claeys, P., Grajales-Nishimura, J.M., and Bermudez, J., 1996, Coarse-grained, clastic sandstone complex at the K/T boundary around the Gulf of Mexico: Deposition by tsunami waves induced by the Chicxulub impact? *in* Ryder, G., Fastovsky, D., and Gartner, S., eds., The Cretaceous-Tertiary Event and Other Catastrophes in Earth History: Geological Society of America Special Paper 307, p. 151–182.
- Vega, F.J., Perrilliat, M.C., Ocampo, A., and Pope, K., 2001, Aporrhaid gastropod of latest Cretaceous age from the upper part of the Barton Creek Formation below Chicxulub ejecta blanket in southern Mexico: VII North American Paleontological Convention, Program and Abstracts, p. 129.
- Warme, J.E., Morgan, M., and Kuehner, H.-C., 2002, Impact-generated carbonate accretionary lapilli in Late Devonian Alamo Breccia, *in* Koeberl, C., and MacLeod, K.G., eds., Catastrophic Events and Mass Extinctions: Impacts and Beyond: Geological Society of America Special Paper 356, p. 489–504.
- Witzke, B.J., and Anderson, R.R., 1996, Sedimentary-clast breccias of the Manson impact structure, *in* Koeberl, C., and Anderson, R.R., eds., The Manson Impact Structure: Geological Society of America Special Paper 302, p. 115–144.
- Wohletz, K.H., and Sheridan, M.F., 1983, Martian rampart crater ejecta: Experiments and analysis of melt-water interaction: Icarus, v. 56, p. 15–37, doi: 10.1016/0019-1035(83)90125-2.